Inelastic neutron scattering study of the multipolar order parameter in NpO_2

N. Magnani,[1,*] S. Carretta,[2] R. Caciuffo,[1] P. Santini,[2] G. Amoretti,[2] A. Hiess,[3] J. Rebizant,[1] and G. H. Lander[1]
[1]*European Commission, Joint Research Centre, Institute for Transuranium Elements, Postfach 2340, D-76125 Karlsruhe, Germany*
[2]*Dipartimento di Fisica, Università di Parma, Viale G. P. Usberti 7/A, I-43100 Parma, Italy*
[3]*Institut Laue-Langevin, Boîte Postale 156, F-38042 Grenoble, France*
(Received 4 August 2008; published 30 September 2008)

We have performed polarized inelastic neutron scattering experiments in the ordered phase of neptunium dioxide. The observation of magnetic scattering between 11 and 18 meV can be attributed to a transition between two states with the same expectation value of the electric quadrupole but opposite values of the magnetic triakontadipole. In contrast to resonant x-ray scattering, which detects the secondary order parameter (electric quadrupoles) associated with the 25 K phase transition, the results reported here are a manifestation of the primary (magnetic) order parameter. The experimental observations are discussed in relation to the current theoretical understanding of the low-energy magnetic dynamics of NpO_2.

DOI: 10.1103/PhysRevB.78.104425 PACS number(s): 78.70.Nx, 75.10.Dg, 75.40.Cx, 75.40.Gb

I. INTRODUCTION

The peculiar low-temperature properties of NpO_2 have kept physicists puzzled for more than half a century. The large anomalies observed at $T_0=25$ K in specific-heat[1] and magnetic-susceptibility measurements[2] were initially thought to be a consequence of antiferromagnetic order, mainly due to the similarity with the behavior of UO_2; however, both neutron diffraction and Mössbauer spectroscopy failed to detect any ordered moment in NpO_2, with an estimated uncertainty of about $0.01\mu_B$. Attempts to associate this "hidden order" with the most obvious nondipolar order parameter (OP), i.e., electric quadrupoles,[3] were initially unsuccessful, since no evidence of static distortions of the oxygen sublattice driven by quadrupolar interactions (as those observed in UO_2) was found.[4,5] Moreover, the appearance of a spontaneous muon precession signal in muon spin resonance (μSR) experiments for $T<T_0$ was a clear indication that the primary order parameter breaks time-reversal symmetry.[6]

Major steps forward in understanding the NpO_2 phase transition were the proposal that a magnetic octupole was a potential OP (Ref. 7) and the resonant x-ray scattering (RXS) experiments showing that the Np electric quadrupoles are indeed ordered below 25 K.[8,9] The RXS observations are compatible with electric quadrupoles as the secondary OP, induced by magnetic multipoles (MMP) of Γ_5 symmetry as the primary OP. The quadrupole motif corresponds to a longitudinal 3-**k** structure that preserves the overall cubic symmetry. After the controversy over the true crystal-field (CF) potential at the Np sites[10] was resolved,[11] the correct primary OP was suggested to be a rank-5 triakontadipole.[12] The ordering of these magnetic multipoles would give rise to the spatial magnetic-field distribution shown in Fig. 1. We stress that the primary OP in NpO_2 has not yet been observed by a direct experiment, although it is suggested by a combination of indirect measurements.

In the work reported here, we have successfully observed a dynamical signature of the primary multipolar OP in NpO_2 by inelastic neutron scattering (INS) on a powder sample; in a mean-field (MF) scheme, an ordering of Γ_5 triakontadipoles implies a lowering of the symmetry to D_{3d} and a splitting of the four-degenerate crystal-field Γ_8 ground state into a Γ_4 doublet and a pair of time-reversal-related Γ_5 and Γ_6 singlets (see Fig. 2). The Γ_5 and Γ_6 states are degenerate in the presence of time-reversal invariance, whereas their degeneracy is removed when time reversal is broken. Whether and how this actually occurs can be directly checked by INS. In fact, the $\Gamma_5\rightarrow\Gamma_4$ and $\Gamma_5\rightarrow\Gamma_6$ transitions are both dipole allowed. Therefore, if only the Γ_5 quadrupolar order detected by RXS (Refs. 8 and 9) and nuclear-magnetic resonance (NMR) (Ref. 13) took place, the Γ_8 quartet would split in a pair of Kramers doublets and a single MF magnetic transition would exist (which physically corresponds to changing the charge-density character from oblate to prolate along $\langle 111\rangle$). On the contrary, if a hidden order of Γ_5 MMP is driving the observed quadrupolar order, the Γ_8 quartets should split in three levels and the spectra should consist of two MF magnetic transitions, which physically correspond to concurrent changes in the local magnetization and charge densities (a lowest energy one, involving the Γ_4 excited doublet, where one Np ion has its electric-quadrupole moment reversed and a vanishing triakontadipole moment, and a higher energy one, $\Gamma_5\rightarrow\Gamma_6$, where the ground and excited states have the same electric quadrupole but a reversed magnetic triakontadipole). Each MF transition produces dispersive exciton branches centered around the bare MF energy which in a powder spectrum will appear as a broad signal, whose fine structure depends on the detailed dispersion relations.[12] Here, we report compelling evidence for a structured magnetic signal originating from the branches associated with the $\Gamma_5\rightarrow\Gamma_6$ transition and so confirming the magnetic multipolar nature of the order parameter.

II. EXPERIMENTAL DETAILS AND RESULTS

The INS experiments with uniaxial polarization analysis were performed on the thermal-neutron triple-axis spectrometer IN20 at the Institut Laue-Langevin. About 11 g of NpO_2 powder was encapsulated in aluminum as a thin plate of about 4 mm thickness. Heusler crystals (Cu_2MnAl) were used as a polarizing monochromator and analyzer, in doubly focusing geometry, with a pyrolytic graphite filter to elimi-

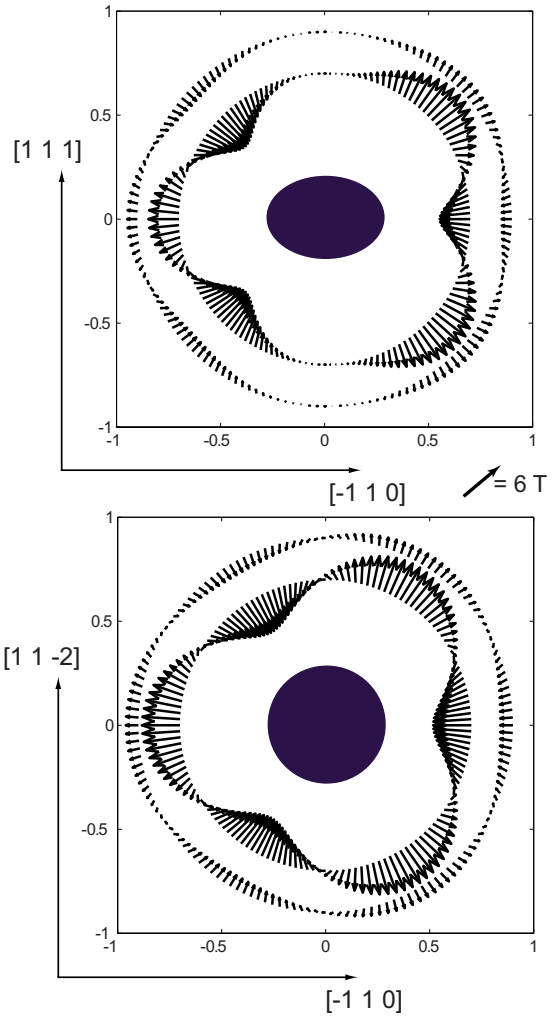

FIG. 1. (Color online) Magnetic field produced by the rank-5 component of the OP of NpO_2 at $T=0$. The Np ion at the center belongs to the sublattice characterized by a magnetic-multipole moment having (111) as the C_3 axis. The field has been calculated at distances of 0.7 and 0.9 Å from the Np nucleus as described by Santini and Amoretti (Ref. 28). The central ellipse schematically represents the quadrupole contribution to the charge density of the $5f$ electrons, which is oblate with respect to the (111) axis.

nate higher-order contaminations of the scattered beam. Data were collected in the constant-Q mode, with fixed final energy $E_f=14.6$ meV ($k_f=2.662$ Å^{-1}). The instrument energy-transfer resolution was about 1.5 meV; the initial polarization was $P_i=0.82(1)$. A flat-coil dc neutron spin flipper was used to reverse the polarization of the incident beam. A system of Helmholtz coils[14] was used to control the direction of the neutron spin at the sample position either parallel to the scattering vector $\mathbf{Q}=\mathbf{k}_i-\mathbf{k}_f$ (horizontal field, HF) or along the vertical direction (vertical field, VF). In the following, the x axis of the reference frame is defined to be parallel to $\mathbf{Q}$, the y axis is perpendicular to $\mathbf{Q}$ and lies in the scattering plane, and the vertical z axis is perpendicular to the scattering plane.

The generalized expression for the neutron cross section can be found in Refs. 15 and 16. If the incident neutron

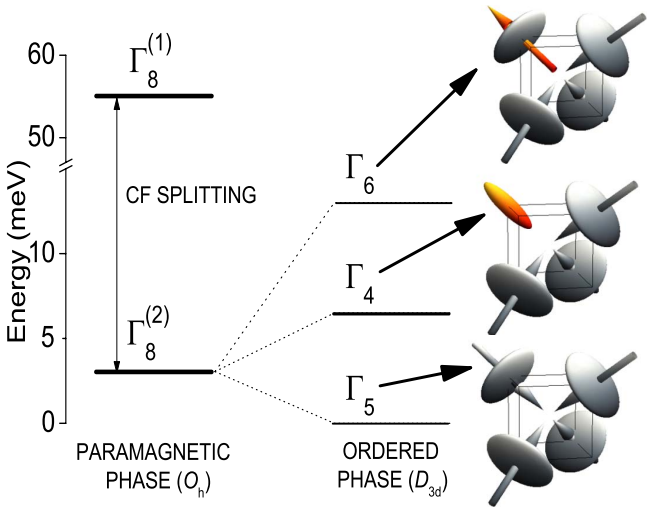

FIG. 2. (Color online) Schematic energy spectra of the Np^{4+} ions in NpO_2. A bare crystal-field gap of 55 meV is present between the two Γ_8 quartets in the paramagnetic phase, with a further Γ_6 excited doublet presumably located about 274 meV above the ground state. In the ordered phase, the ground CF quartet is split into two $\Gamma_{5,6}$ singlets, having the same expectation value for the electric quadrupole (represented by an ellipsoid) but reversed magnetic triakontadipole (represented by an arrow), and a Γ_4 doublet, having reversed electric quadrupole with respect to the $\Gamma_{5,6}$ states and null magnetic triakontadipole.

polarization $\mathbf{P}_i$ is parallel to $\mathbf{Q}$, the polarization component P_{fx} of the scattered beam is given by

$$P_{fx}\sigma = a + NN^*P_i - (M_{\perp y}M^*_{\perp y} + M_{\perp z}M^*_{\perp z})P_i, \qquad (1)$$

where σ is the double-differential cross section, a is a polarization-independent background, N indicates the vibrational scattering amplitude, and $M_{\perp\alpha}$ are Cartesian components of the inelastic neutron magnetic scattering operator. A chiral magnetic term is ignored, as the system considered here is cubic and centrosymmetric. The scattering from lattice vibrations, proportional to NN^*, then gives rise to a non-spin-flip (NSF) signal, whereas magnetic scattering reverses the polarization of the beam, and hence leads to a spin-flip (SF) signal. On the other hand, with $\mathbf{P}_i$ parallel to z the final polarization along the vertical direction is such that

$$P_{fz}\sigma = a + NN^*P_i + (M_{\perp z}M^*_{\perp z} - M_{\perp y}M^*_{\perp y})P_i. \qquad (2)$$

In this configuration, components of the magnetic fluctuation perpendicular to $\mathbf{Q}$ but parallel to $\mathbf{P}_i$ give rise to NSF scattering, whereas components perpendicular to both $\mathbf{Q}$ and $\mathbf{P}_i$ produce SF scattering. For a polycrystalline sample, the response is isotropic and therefore the purely magnetic scattering can be determined either by comparing SF (flipper on) and NSF (flipper off) intensities in the HF mode or as twice the difference between HF and VF spin-flip count rates $2(I^{\mathrm{HF}}_{\mathrm{SF}}-I^{\mathrm{VF}}_{\mathrm{SF}})$. The background is given by $2I^{\mathrm{VF}}_{\mathrm{SF}}-I^{\mathrm{HF}}_{\mathrm{SF}}$.

In the energy window between 3 and 11 meV, a single broad peak at about 6.4 meV had been identified by previous INS experiments on powder samples.[10] Low-T specific-heat measurements[17] are inconsistent with the presence of excited

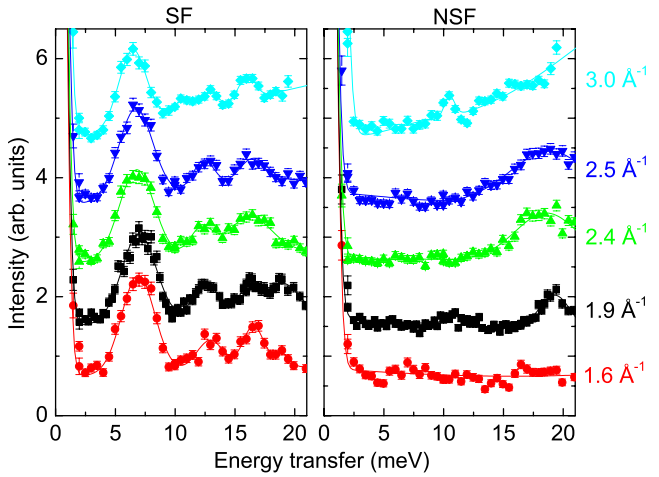

FIG. 3. (Color online) Q dependence of the spin-flip (left panel) and non-spin-flip (right panel) INS spectra of a NpO_2 powder sample. Data were collected with the sample kept at $T=5$ K and incident polarization parallel to **Q**. Lines are guides for the eyes. A vertical offset of 0.1 is applied to each spectrum for clarity.

levels below 3 meV in the ordered phase. Therefore, if further signal originating from a second MF transition exists, it has to be sought above 11 meV.

INS spectra measured at $T=5$ K with initial polarization parallel to **Q** are shown in Fig. 3 for different Q values. A comparison of SF spectra (magnetic signal) and NSF spectra (nuclear incoherent and phonon contributions) clearly shows that additional magnetic scattering is indeed present between 11 and 18 meV. By measuring INS spectra for $Q=1.9$ Å^{-1} at different temperatures, we establish that its intensity decreases as the temperature increases (Fig. 4); therefore, we attribute these features to the sought-after $\Gamma_5 \rightarrow \Gamma_6$ transition. The magnetic signal, however, does not completely disappear in the paramagnetic phase; this is consistent with earlier observations[10] and may be attributed to short-range order or

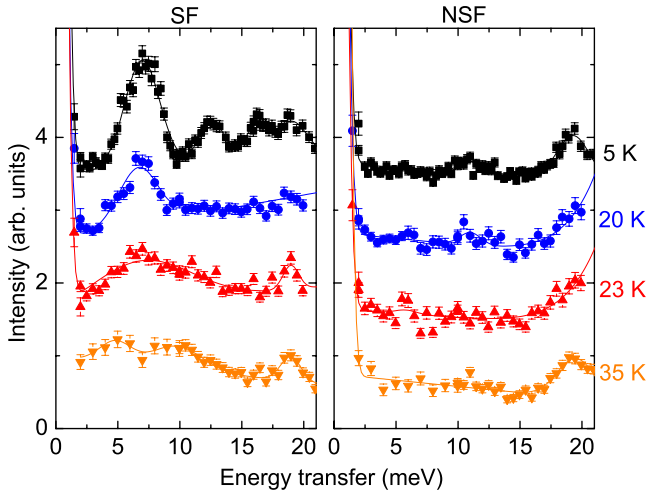

FIG. 4. (Color online) Temperature dependence of the spin-flip (left panel) and non-spin-flip (right panel) INS spectra of a NpO_2 powder sample. Data taken at $Q=1.9$ Å^{-1}, with incident polarization parallel to **Q**. Lines are guides for the eyes. A vertical offset of 0.1 is applied to each spectrum for clarity.

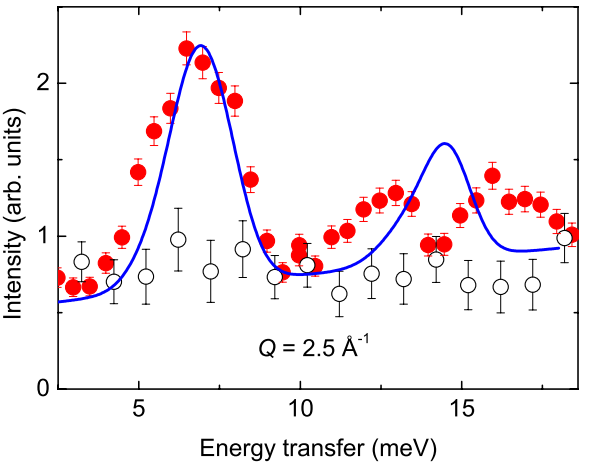

FIG. 5. (Color online) Full dots: spin-flip INS spectra at $Q=2.5$ Å^{-1} and $T=5$ K, with incident polarization parallel to **Q**. Open dots: nonmagnetic background, estimated as the difference between twice the SF intensity in the VF configuration and the SF intensity in the HF configuration. Line: calculated RPA spectra for $Q=2.5$ Å^{-1} convoluted with a Gaussian resolution function of 1.5 meV.

Jahn-Teller phenomena. In any case, a residual splitting above the transition temperature is compatible with specific-heat measurements which demonstrate that the full magnetic entropy of the ground-state quartet is not recovered at T_0 (Ref. 17); this is similar to observations made for UO_2.[18] In the ordered phase, the temperature dependence of the lowest energy peak was already reported in Ref. 10. As seen from Fig. 4 the statistics on the higher energy signal do not warrant such a detailed analysis due to its lower intensity.

As shown in Fig. 3, for $Q<2$ Å^{-1} the NSF spectra are quite clean in the region of interest (i.e., below 18 meV) and therefore can be taken as a good estimate of the polarization-independent background. For higher values of Q, a structured nonmagnetic contribution is clearly present in the NSF channel below 18 meV; a comparison with the phonon density of states reported for UO_2 (see, for example, Ref. 19) allows one to attribute this signal to the transverse-acoustic and longitudinal-acoustic phonon branches. To estimate the background correctly in these cases we have measured the spin-flip INS spectra at $Q=2.5$ Å^{-1} with the initial neutron polarization perpendicular to the scattering plane. In this configuration, the spin-flip intensity is given by the sum of the background (nuclear incoherent and vibrational scattering) and half of the magnetic signal, and the background is readily obtained as $2I_{SF}^{VF}-I_{SF}^{HF}$ (Fig. 5).

A survey of the experimental data collected here shows that the powder signal observed above 11 meV is structured in two separate peaks, whereas a static mean-field model predicts the presence of a single peak associated with the triakontadipole transition. Within the resolution of the experiment, the splitting between the two peaks does not change when Q varies from 1.6 to 3.0 Å^{-1} (Fig. 3). On the other hand, the ground Γ_8 quartet of NpO_2 cannot be split further without breaking the D_{3d} symmetry established by RXS.[5,8]

To compare the experimental results with theoretical predictions it is necessary to take into account the **Q** dispersion

of the mean-field modes induced by the superexchange coupling. This dispersion depends on the direction of the **Q** vector and an angular average must be performed to account for the polycrystalline nature of the sample. Section III describes the adopted calculation procedure, which follows the random-phase approximation (RPA) analysis outlined in Ref. 12, and the comparison of the obtained results with the experiment.

III. DISCUSSION

A. Dynamical susceptibility

In the 3-**k** ordered phase of NpO_2, the Np^{4+} ions occupy four inequivalent sublattices ($s=1,\ldots,4$), each one corresponding to a different orientation of the MMP moment. The effective single-ion Hamiltonian is the sum of crystal-field and mean-field contributions, $H(s)=H_J+H_{\mathrm{mix}}+H_{\mathrm{MF}}(s)$, where H_J is the cubic crystal field acting on the ground J multiplet, H_{mix} is a second-order perturbative term describing J-mixing effects,[11] and $H_{\mathrm{MF}}(s)$ contains the contributions of rank-5 magnetic-multipole and electric-quadrupole order parameters.[12] The single-ion cross susceptibilities $\chi_{AB}^{\alpha,\beta}$ for observables A_α and B_β ($\alpha,\beta=x,y,z$) can be calculated by self-consistent diagonalization of $H(s)$. The dynamical susceptibilities are then obtained by including fluctuations with a RPA approach. The most general model contains a large number of parameters, even if nearest-neighbor coupling only is assumed. This number could be reduced by considering only the ground Γ_8 quartet states, an approximation which makes many multipoles proportional to one another. However, even in this case, as many as 24 parameters remain allowed by the bond symmetry (18 describing magnetic couplings and 6 associated with electric ones).

If the quadrupolar contribution to $H_{\mathrm{MF}}(s)$ is neglected, the RPA system involves the lowest possible number of multipoles, namely, three magnetic-dipole and three rank-5 multipole degrees of freedom for each of the four sublattices. A 24×24 system must therefore be solved,

$$dJ_\alpha(\mathbf{q},E)=\sum_\beta \chi_{JJ}^{\alpha,\beta}dH_{\mathrm{ext}}^{\beta}[\mathbf{q}+\mathbf{q}_{\mathrm{AF}}(\alpha,\beta),E]+\sum_{\beta,\gamma}\chi_{JJ}^{\alpha,\beta}I_J^{\beta,\gamma}[\mathbf{q}+\mathbf{q}_{\mathrm{AF}}(\alpha,\beta)]dJ_\gamma[\mathbf{q}+\mathbf{q}_{\mathrm{AF}}(\alpha,\beta),E]$$
$$+\sum_{\beta,\gamma}\chi_{JO}^{\alpha,\beta}I_O^{\beta,\gamma}[\mathbf{q}+\mathbf{q}_{\mathrm{AF}}(\alpha,\beta)]dO_\gamma[\mathbf{q}+\mathbf{q}_{\mathrm{AF}}(\alpha,\beta),E], \tag{3}$$

$$dO_\alpha(\mathbf{q},E)=\sum_\beta \chi_{OJ}^{\alpha,\beta}dH_{\mathrm{ext}}^{\beta}[\mathbf{q}+\mathbf{q}_{\mathrm{AF}}(\alpha,\beta),E]+\sum_{\beta,\gamma}\chi_{OO}^{\alpha,\beta}I_O^{\beta,\gamma}[\mathbf{q}+\mathbf{q}_{\mathrm{AF}}(\alpha,\beta)]dO_\gamma[\mathbf{q}+\mathbf{q}_{\mathrm{AF}}(\alpha,\beta),E]$$
$$+\sum_{\beta,\gamma}\chi_{OJ}^{\alpha,\beta}I_J^{\beta,\gamma}[\mathbf{q}+\mathbf{q}_{\mathrm{AF}}(\alpha,\beta)]dJ_\gamma[\mathbf{q}+\mathbf{q}_{\mathrm{AF}}(\alpha,\beta),E]. \tag{4}$$

In the above equations, $H_{\mathrm{ext}}^{\beta}(\mathbf{q},E)$ is the external magnetic field and $I_A^{\alpha,\beta}(\mathbf{q})$ is the Fourier transform of two-ion couplings between observables A_α and A_β. Finally, $\mathbf{q}_{\mathrm{AF}}(\alpha,\beta)$ is equal to zero for $\alpha=\beta$, whereas $\mathbf{q}_{\mathrm{AF}}(\alpha,\beta)=\mathbf{k}_\gamma$ if $\alpha\neq\beta$, with $\gamma\neq\alpha,\beta$ and $\mathbf{k}_x=2\pi/a(100)$, etc. If only nearest-neighbor coupling is considered, the model has six independent parameters. A further simplification is obtained by assuming isotropic dipole-dipole couplings $I_J^{\alpha,\beta}$, and the same form for $I_O^{\alpha,\beta}$. In this way, the number of free parameters is reduced to two, namely, the dipole-dipole (I_J^0) and triakontadipole-triakontadipole (I_O^0) interactions. These two parameters can be determined from the static magnetic susceptibility in the paramagnetic phase ($I_J^0\simeq 0.1$ meV) and from the energy of the $\Gamma_5\rightarrow\Gamma_4$ INS transition ($I_O^0=4.9\times 10^{-7}$ meV). Calculations with a larger number of input parameters are cumbersome and highly nonunivocal in the lack of detailed information on dispersion relations from single-crystal experiments.

B. Comparison with experimental data

The powder-averaged INS spectrum calculated for $Q=2.5$ Å^{-1} is shown in Fig. 5, where it is superimposed to the experimental data. The calculated signal arising from the $\Gamma_5\rightarrow\Gamma_6$ transition is a single peak with slightly asymmetric shape instead of two separate peaks as experimentally observed. However, the fact that the overall experimental magnetic intensity integrated from 11 to 18 meV compares well with the calculated one is a hint that the full magnetic signal within this energy range should be attributed to the triakontadipole reversal.

To further check this assumption, we compare the intensity ratio of the total signal in the range 11–18 meV to the signal at 7 meV. This ratio is plotted as a function of the momentum transfer Q in Fig. 6. If we assume that the 7 meV peak corresponds to the $\Gamma_5\rightarrow\Gamma_4$ transition and that the intensity at higher energy is due to the $\Gamma_5\rightarrow\Gamma_6$ transition a single-ion model would predict this ratio to be constant because the intensity of both transitions would simply be proportional to the square of the dipolar form factor $f(Q)$. On the other hand, superexchange interactions trigger a dispersive behavior of these excitations, which is evidenced as a Q dependence of the peak intensities in the powder INS spectra. The observed ratio is in very good agreement with the one calculated by our RPA model (Fig. 6) and we stress again that, once I_J^0 and I_O^0 are fixed to reproduce the experimental paramagnetic sus-

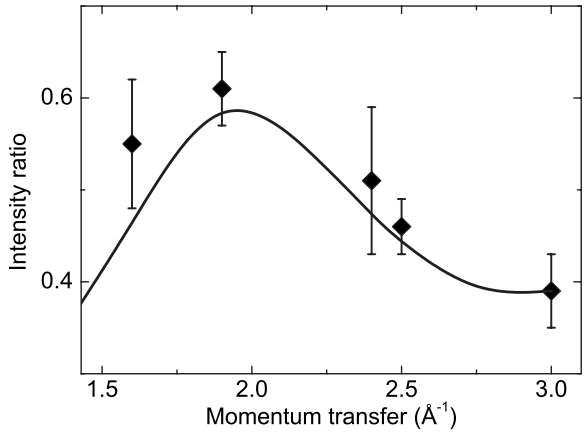

FIG. 6. Experimental (diamonds) and calculated (line) Q dependences of the ratio between the magnetic scattering intensity of the $\Gamma_5 \rightarrow \Gamma_6$ transition and that of the $\Gamma_5 \rightarrow \Gamma_4$ transition for a powder sample.

ceptibility and the quadrupolar transition energy, no free parameters remain. This demonstrates that, despite the remaining discrepancies, this simple model already allows us to correctly appreciate the general physical picture.

A more careful inspection of the calculations actually allows us to formulate a possible explanation for the observed double-peak structure. The asymmetry of the calculated $\Gamma_5 \rightarrow \Gamma_6$ peak arises from the angular average of two intense branches of which only one is visible for $\mathbf{Q}$ along $\langle 001 \rangle$. For a generic direction of $\mathbf{Q}$ the two branches are separate, as shown in Fig. 7. Thus, it is likely that the two observed high-E peaks originate from an energy separation of these two branches larger than that predicted by our simplified model. This might be quantitatively reproduced if the values of all the superexchange coupling parameters were known. We state once again that their number is so large that, even if we were able to measure the full dispersion curves of a single crystal, this may not be informative enough and that in any case most of the interesting physics is already contained in the simplest model (at least qualitatively). For the sake of completeness, it is worth recalling that magnon-phonon interactions are important in actinide dioxides (such as UO_2) (Refs. 10, 18, and 20–22) and might also affect the details of the present excitations.

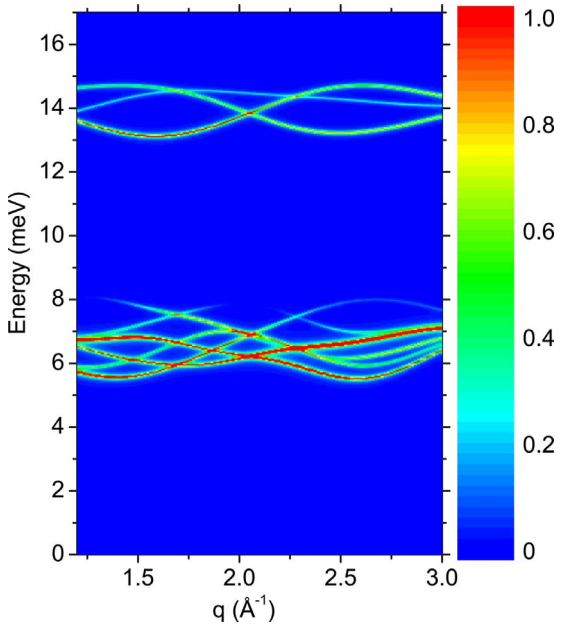

FIG. 7. (Color online) Intensity plot showing the calculated $T=0$ momentum transfer and energy dependence of the neutron scattering function along the generic nonsymmetry direction $\mathbf{Q}=q(0.167\ 0.514\ 0.841)$. The color scale on the right-hand side represents the scattering intensity in arbitrary units.

IV. CONCLUSIONS

Inelastic neutron scattering experiments performed on polycrystalline NpO_2 have allowed considerable progress in elucidating the ground state of this fascinating compound. In earlier work[10] a splitting of the Γ_8 state was observed and its quadrupolar nature was identified; following a number of different experiments with both NMR and RXS, theory predicted that a second allowed transition between the Γ_5 ground state and a Γ_6 excited state should exist,[12] associated with a change in sign of the expectation value of the hidden primary order parameter (Fig. 2). This has been directly observed by the present experiment.

Whereas both the overall energy range and the intensity of the observed resonance are in agreement with those expected by a RPA dynamic susceptibility calculation with a minimal number of parameters,[12] the observed splitting of the MF $\Gamma_5 \rightarrow \Gamma_6$ transition cannot be completely reconciled with such a theory, most likely due to the fact that more complex multipolar couplings have to be included in the model. To clarify this point further, detailed information about the actual fine structure of the two-ion multipolar interactions should be obtained, for example, by fully measuring the dispersion of the low-energy modes on a NpO_2 single crystal; however, due to the absence of large single crystals and despite the improving experimental possibilities of neutron instruments in terms of data-collection rate, such an experiment is unlikely to become feasible in the near future.

Neutron diffraction could, in principle, be used for an even more direct measurement of the triakontadipolar magnetic field (Fig. 1), as recently demonstrated in a study of magnetic octupole order in $Ce_{0.7}La_{0.3}B_6$.[23] In fact, whereas magnetic superlattice reflections associated with dipolar order have an intensity that rapidly falls to zero as the momentum transfer Q increases, Bragg peaks due to ordered higher-order magnetic multipoles have maximum intensity at nonzero Q values. This difference in the Q dependence of the intensity would provide a clear identification of the OP. However, all attempts to grow large enough single crystals of NpO_2 have been unsuccessful despite the possibility to do so with similar compounds such as UO_2 (Ref. 18); this is the main reason which prevents such a study from being performed. Another potential microscopic probe of magnetic-multipole order is NMR, which is sensitive to the magnetic field at the ligand site through the hyperfine interaction with the nuclear spins.[24,25] Measurements on ^{17}O enriched samples gave additional indirect evidence for the existence

of a longitudinal 3-**k** multipole order in NpO_2.[13,26] Field-angle-resolved ^{17}O-NMR results on a single crystal of NpO_2 was used to address the multiple hyperfine field components individually and evidenced the field-induced magnetic-dipole and multipole moments arising from the secondary antiferroquadrupolar order. However, direct contributions from Np magnetic multipoles in zero field are not accessible as they vanish by symmetry at the oxygen sites.[27] Doping with Th could eventually perturb this cancellation, giving the opportunity to detect the resultant multipolar field.

ACKNOWLEDGMENTS

We gratefully acknowledge help from the technical staff of the Institut Laue-Langevin, who addressed all the safety concerns related to this transuranium experiment.

*nicola.magnani@ec.europa.eu

[1] D. W. Osborne and E. F. Westrum, J. Chem. Phys. **21**, 1884 (1953).
[2] J. W. Ross and D. J. Lam, J. Appl. Phys. **38**, 1451 (1967).
[3] P. Morin and D. Schmitt, in *Ferromagnetic Materials*, edited by K. H. J. Buschow and E. P. Wohlfarth (Elsevier, Amsterdam, 1990), Vol. 5, pp. 1–132.
[4] R. Caciuffo, G. H. Lander, J. C. Spirlet, J. M. Fournier, and W. F. Kuhs, Solid State Commun. **64**, 149 (1987).
[5] D. Mannix, G. H. Lander, J. Rebizant, R. Caciuffo, N. Bernhoeft, E. Lidstrom, and C. Vettier, Phys. Rev. B **60**, 15187 (1999).
[6] W. Kopmann, F. J. Litterst, H.-H. Klauss, M. Hillberg, W. Wagener, G. M. Kalvius, E. Schreier, F. J. Burghart, J. Rebizant, and G. H. Lander, J. Alloys Compd. **271-273**, 463 (1998).
[7] P. Santini and G. Amoretti, Phys. Rev. Lett. **85**, 2188 (2000).
[8] J. A. Paixao, C. Detlefs, M. J. Longfield, R. Caciuffo, P. Santini, N. Bernhoeft, J. Rebizant, and G. H. Lander, Phys. Rev. Lett. **89**, 187202 (2002).
[9] R. Caciuffo, J. A. Paixao, C. Detlefs, M. J. Longfield, P. Santini, N. Bernhoeft, J. Rebizant, and G. H. Lander, J. Phys.: Condens. Matter **15**, S2287 (2003).
[10] G. Amoretti, A. Blaise, R. Caciuffo, D. Di Cola, J. M. Fournier, M. T. Hutchings, G. H. Lander, R. Osborn, A. Severing, and A. D. Taylor, J. Phys.: Condens. Matter **4**, 3459 (1992).
[11] N. Magnani, P. Santini, G. Amoretti, and R. Caciuffo, Phys. Rev. B **71**, 054405 (2005).
[12] P. Santini, S. Carretta, N. Magnani, G. Amoretti, and R. Caciuffo, Phys. Rev. Lett. **97**, 207203 (2006).
[13] Y. Tokunaga *et al.*, Phys. Rev. Lett. **97**, 257601 (2006).
[14] The ILL Yellow Book, 2005 (http://www.ill.fr).
[15] M. Blume, Phys. Rev. **130**, 1670 (1963).
[16] S. V. Maleyev, V. G. Bar'yakhtar, and R. A. Suris, Sov. Phys. Solid State **4**, 2533 (1963).
[17] N. Magnani, P. Santini, G. Amoretti, R. Caciuffo, P. Javorský, F. Wastin, J. Rebizant, and G. H. Lander, Physica B (Amsterdam) **359-361**, 1087 (2005).
[18] R. Caciuffo, G. Amoretti, P. Santini, G. H. Lander, J. Kulda, and P. de V. Du Plessis, Phys. Rev. B **59**, 13892 (1999).
[19] G. Dolling, R. A. Cowley, and A. D. B. Woods, Can. J. Phys. **43**, 1397 (1965).
[20] E. Blackburn, R. Caciuffo, N. Magnani, P. Santini, P. J. Brown, M. Enderle, and G. H. Lander, Phys. Rev. B **72**, 184411 (2005).
[21] R. A. Cowley and G. Dolling, Phys. Rev. **167**, 464 (1968).
[22] J. M. Fournier, A. Blaise, G. Amoretti, R. Caciuffo, J. Larroque, M. T. Hutchings, R. Osborn, and A. D. Taylor, Phys. Rev. B **43**, 1142 (1991).
[23] K. Kuwahara, K. Iwasa, M. Kohgi, N. Aso, M. Sera, and F. Iga, J. Phys. Soc. Jpn. **76**, 093702 (2007).
[24] O. Sakai, R. Shiina, H. Shiba, and P. Thalmeier, J. Phys. Soc. Jpn. **66**, 3005 (1997).
[25] R. Shiina, O. Sakai, H. Shiba, and P. Thalmeier, J. Phys. Soc. Jpn. **67**, 941 (1998).
[26] Y. Tokunaga, Y. Homma, S. Kambe, D. Aoki, H. Sakai, E. Yamamoto, A. Nakamura, Y. Shiokawa, R. E. Walstedt, and H. Yasuoka, Phys. Rev. Lett. **94**, 137209 (2005).
[27] O. Sakai, R. Shiina, and H. Shiba, J. Phys. Soc. Jpn. **74**, 457 (2005).
[28] P. Santini and G. Amoretti, J. Phys. Soc. Jpn. **71** Suppl., 11 (2002).